

# A quantitative study between HPGR and cone crusher aided ball mill grinding: mathematical modeling by evaluating the possible microfracture effect produced by HPGR technology and cone crusher

I. Rodríguez-Torres <sup>1</sup>, E.T. Tuzcu <sup>2</sup>, Iván A. Reyes <sup>1</sup>, G. Rosales-Marín <sup>1,3</sup>

<sup>1</sup> Facultad de Ingeniería - Instituto de Metalurgia, Universidad Autónoma de San Luis Potosí, México

<sup>2</sup> MPES Engineering, Elmar Towers C Block, 3028. Cad. No: 8C Kat: 19 Daire: 200, Konutkent Mah, 06810 Ankara, Turkey.

<sup>3</sup> Unidad Académica Multidisciplinaria Región Altiplano, Ingeniería de Minerales, Universidad Autónoma de San Luis Potosí, México

Corresponding author: gilberto.rosales@uasl.mx (G. Rosales-Marín)

**Abstract:** High Pressure Grinding Rolls (HPGR) have been used in the mining industry for decades. However, there are limited quantifications of the particle properties after comminution. Furthermore, the influence of microcracks in grinding provided by this technology has not been extensively quantified. In the recent work, there were two comminution paths tested: 1 (Jaw crusher + cone crusher + ball mill) and 2 (Jaw crusher + HPGR + ball mill). The possible weakening effect aiding ball mill grinding due to microcracks of HPGR path was shown via specific energy, fines generation and breakage rate measurements. To achieve a quantification about the impact of microcracks and the high rate of reduction rate of HPGR technology, first the product was reconstructed using Rosin Rammler's Weibull double formula and the similar particle size distribution was obtained by a conventional cone crusher. By this way the feed size distribution to the grinding stage remained constant regardless of the type of crushing process (HPGR or cone crusher). The results showed that the microfractures generated by the HPGR technology influence the specific energy consumption, fines generation and breakage rates. Ball mill after HPGR consumed 12.46 kWh/t of specific energy, however ball mill after cone crusher consumed 14.36 kWh/t of specific energy. The experimental methodology proposed in this paper maintains a consistent feed size range (-1500 to +41.31  $\mu\text{m}$ ) to show that the size reduction observed in the sample undergoing HPGR grinding is not the primary factor contributing to reduced energy consumption and increased fines generation. Instead, it is predominantly associated with the microfractures generated through the compression in HPGR technology; the energy reduction (optimization) of a grinding path is shown in the study.

**Keywords:** high pressure grinding rolls, cone crusher, mathematical modeling, comminution, mineral processing

## 1. Introduction

In today's world, the decrease in ore head grade and having finer dissemination in most of the strategic ores have brought difficulties in ore processing. Comminution, a pivotal phase in ore preparation, centers on reduction of particle sizes to optimize mineral liberation. HPGR technology was first introduced into the cement industry in the 80s. It is based on the principle of inter-particle breakage via the ore grain boundaries by applied pressure and results in micro-fracturing the ore. This equipment offers several energy advantages (Schonert, 1988; Dunne et al., 1996; Celik and Oner, 2006). Such as; energy efficiency, improved particle liberation, preventing overgrinding and lower water usage among others. Fujimoto (1993) gave an overview about the technical innovations to reduce the power consumption in cement plants. Other investigations also showed improvements in the beneficiation indicators of ore processing such as: improvement of operational recovery of the ore, significant

reduction in energy consumption of subsequent grinding and obtaining higher proportion of fines products compared to the jaw crusher (Gutsche and Fuerstenau, 2004; Michaelis, 2005; Daniel, 2007). Studies also emerged on the ability of HPGR in terms of higher size reduction ratio compared to capacity, lower grinding media consumption, smaller footprint, less noise, and better adaptability (Maxton et al., 2003; Tavares, 2005; Zhao et al., 2011; Altun et al., 2011; Fan et al., 2012). The impact of microfractures has been thoroughly examined in recent studies conducted by Gao et al. (2019) and Nghipulile et al. (2023). Both investigations conclusively demonstrate the discernible influence of High-Pressure Grinding Roller (HPGR) and Conventional Crushing methods on the proliferation of microcracks. Specifically, the studies illuminate the consequential effects of these techniques on enhancing the liberation degree of vanadium-titanium magnetite and Platinum Ore, respectively, with a noteworthy emphasis on the advancements facilitated by HPGR technology.

### 1.1. Particle damage characterization in comminution processes

In their works, Miller and Lin (2009), and Lin and Miller (2010) and Dhawan, et. al., (2012) illustrated the impact of various comminution methods on particle damage and breakage energy, utilizing a copper ore. In a study conducted by Miller et al. (2009), high-resolution X-ray imaging was employed to discern the extent of crack damage (Fig. 1). Their findings highlighted that utilization of HPGR technology led to greater formation of cracks, further emphasizing its effectiveness in enhancing mineral liberation.

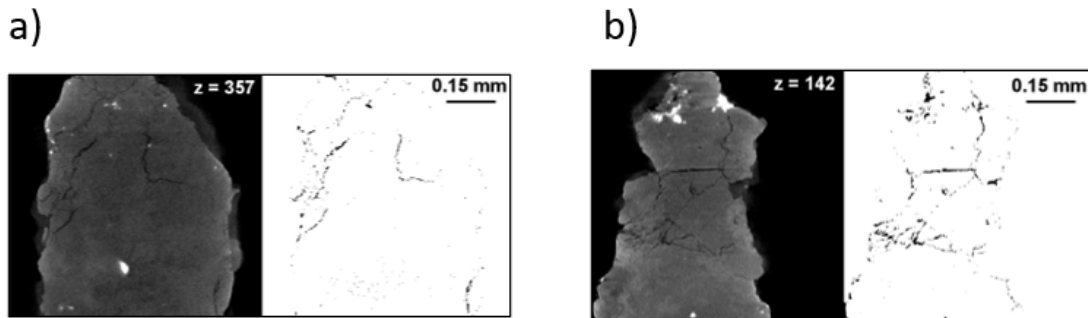


Fig. 1. Internal crack, between a) JAW Crusher and b) HPGR product (Miller and Lin Recent Advances in Mineral Processing Plant Design, SME (2009))

Lin and Miller (2010) conducted higher resolution particle tomography to analyze internal cracks, pores, and crack surfaces within the products of both Jaw Crusher and HPGR. As depicted in Fig. 2, the HPGR product reveals numerous prominent dark regions, indicative of a substantial level of fractures.

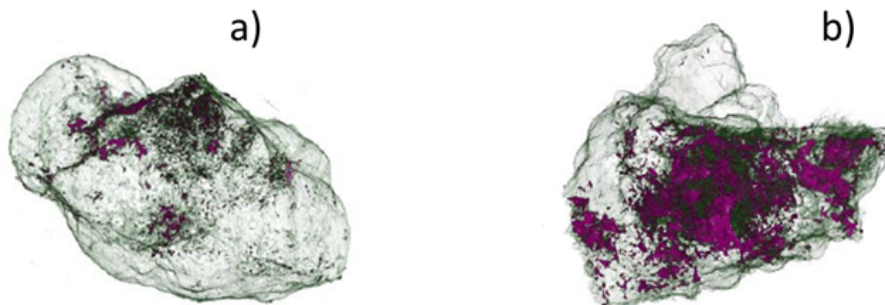


Fig. 2. Internal crack, pores and crack surface between a) JAW Crusher and b) HPGR product (Lin and Miller. SME 2010 Annual Meeting)

While much has been documented in the literature about the effects of HPGR technology, the precise quantification of the real impact of microfractures on key parameters like energy consumption, fracture propagation speed, and fine particle generation has remained a formidable challenge. The objective of this paper is to explore the microfracture assisted finer size distribution by HPGR in grinding against the cone crusher. A copper-silver ore was treated in the experiments. The Rosin Rammler's double

Weibull equation was used to re-create the feed size distribution (independent of HPGR or cone) to a ball mill grinding kinetics test and the population balance model (PBM) was used to evaluate the grindability, energy consumption and fine particles generation.

## 2. Materials and methods

### 2.1. The population balance model (PBM)

The selection and breakage functions are two main components of the batch population balance equation. Breakage functions are determined by grinding tests and selection functions are usually either back calculated or directly estimated from energy studies. The breakage rates are the key parameters for PBM approach. So far, several different approaches for estimation of selection functions have been proposed. Such as: those based on probability of capture and nipping (Nomura et. al., 1991), based on impact energy spectra (Bourgeois, 1993; Datta, 1993; Tavares and Carvalho, 2009; Tuzcu and Rajamani, 2011) and based on probability of breakages (Vogel and Peukert, 2003). However, in this study, the main calculations were made based on Austin and Herbst-Fuerstenau's selection function approaches. In the analysis of the materials breakage, it may be useful to make an initial assumption that the breakage of each size fraction is the first order in nature (Austin, L.G 1982). The selection function is the fractional rate at which a given size of particle is broken into smaller particles. The breakage function is the size distribution of the mother fragments after breakage occurs.

The fundamental logic behind the PBM may be explained as the mass entering to a system must, either leaves the system or accumulates within the system. The PBM is specifically formulated as a numeric balance: *Accumulation = Input – Output + Net Generation*.

This equation shows two principal ways by which individual particles move in the phase space while changing their external and internal coordinates. The size discretized batch PBM is expressed as:

$$\frac{d[H m_i(t)]}{dt} = -S_i(t)H m_i(t) + \sum_{j=1}^{i-1} b_{ij} S_j(t)H m_j(t) \quad (1)$$

where  $b_{ij}$  is the fraction of broken mass of size class  $j$  appearing in size class  $i$ , and  $S_i$  is the fractional rate of breakage of size class  $i$ . If it is assumed that the hold-up is constant, the batch population balance equation becomes:

$$\frac{d[m_i(t)]}{dt} = -S_i(t) m_i(t) + \sum_{j=1}^{i-1} b_{ij} S_j(t)m_j(t) \quad (2)$$

Based on the normalizability assumption:

$$b_{ij} = b_{i-j+1,1} \quad (3)$$

Under this assumption the breakage function for all sizes ( $b_{i2}, b_{i3}, \dots, b_{i,n-1}$ ) are obtained directly from  $b_{i1}$ . The short and very nice PBM explanation is given elsewhere (Bhattacharyya et al, 2016)

The formula used for the variation of the specific rate of breakage  $S_i$  with particle size is:

$$S_i(d) = a \cdot \left[ \frac{X_i}{X_0} \right]^\alpha \cdot Q(x) \quad (4)$$

and  $Q(x)$  correction factor for slow speed breakage is expressed as:

$$Q(x) = \frac{1}{1 + \left[ \frac{X_i}{\mu} \right]^\Lambda} \quad (5)$$

where the fracture speed  $a$  and the material ground parameter  $\alpha$  depends on the material in a mill under defined operating conditions;  $X_i$  is the particle size in mm;  $X_0$  is a reference size, usually 1 mm;  $\mu$  defines the particle size at which  $Q(x)$  is 0.5 and  $\Lambda$  is an index of how rapidly the rate of breakage falls away (Austin et al., 1983). The equation relating the value of the size  $X_m$  (at which the rate of breakage is a maximum for a given material) to the parameter  $\mu$  is as follows:

$$\mu = X_m \left( \frac{\Lambda}{\alpha} - 1 \right)^{\frac{1}{\Lambda}} \quad \text{on condition that } \Lambda > \alpha \quad (6)$$

The specific rate of breakage ( $S_i^F$ ) parameters ( $a$ ,  $\alpha$ ,  $\mu$ , and  $\Lambda$ ) were obtained by back-calculation of (Eq. (2), (Klimpel, 1983). The values were obtained by fitting the parameters by minimizing the error between experimental values ( $P_{exp}(t)$ ) and the predicted ones ( $P_{model}(t)$ , (Katubilwa and Moys, 2009) in this technique. Fig. 8 shows the specific rate of breakage for the HPGR and cone crusher with an SSE

value of 1.02 and 1.05, respectively. The point where the highest breakage occurs is defined by the parameter  $\mu$ . The breakage rate decreases starting from this value.

The parameter  $a$  represents the intersection of the axis of the plot (specific selection function  $S_i^E$  vs particle size) and is directly proportional to the specific rate of breakage expressed in  $\text{time}^{-1}$ . The parameters  $a$  and  $\mu$  depend on the operational conditions (in this case pre grinding in addition to the ball milling). The parameter  $a$  is the slope of the line and is a positive number, usually in the range 0.5–1.5. It is characteristics of the material and does not change with milling conditions (type of lifter, rotational rate, ball load, ball size or mill hold-up) (Austin and Brame, 1983). The value for the parameter  $\Lambda$  was chosen from the literature to initiate the estimation procedure (Austin *et al.*, 1982).

The rate of breakage increases with particle size which reflects the decreasing strength of the particles as the size increases. This is attributed to the greater density of micro flaws in the interior of larger particles and to the greater like hood that a particular large particle will contain a flaw that will initiate fracture under the prevailing stress conditions in a mill. The decrease in particle strength does not lead to an indefinite increase in the specific rate of breakage. As the particle size becomes significant by comparison to the size of the smallest media particles, the prevailing stress levels in the mill are insufficient to cause fracture and the specific rate of breakage passes through a maximum and decreases with further increase in particle size (King, 2001). Herbst and Fuerstenau (1973), Herbs *et al.* (1973) and Herbst and Rajamani (1982) applied the selection function for scaling up through the specific selection function. The specific selection function is proportional to the mass-specific power input to the mill.

$$S_i^E = S_i \frac{M}{P} \quad (7)$$

where  $M$  is the mass of the charge in the mill excluding the media and  $P$  is the basic mill power drawn. The power draw in a mill is related to the torque by:

$$P = \frac{2\pi N\tau}{60} \quad (8)$$

where  $N$  is the mill speed in rpm,  $\tau$  is the torque exerted by the mill minus friction on the bearings. The breakage function ( $b_{ij}$ ) in the PBM Equation 1, can be expressed in functional form as (Austin and Luckie):

$$B_{ij} = \emptyset \left( \frac{x_{i-1}}{x_j} \right)^{\alpha_2} + (1 - \emptyset) \left( \frac{x_{i-1}}{x_j} \right)^{\alpha_3} \quad (9)$$

The  $B_{i,j}$  function describes the size distribution of the fine fraction in the population of progeny particles.  $x_i$  is the top value of the size interval is indexed by  $i$ . Parameters  $\emptyset$ ,  $\alpha_2$  and  $\alpha_3$  are the model parameters to be adjusted from the experimental data.  $B_{ij}$  is the cumulative form of the  $b_{ij}$  function, as shown in Equation 10.

$$b_{ij} = \begin{cases} B_{i,j} - B_{i+1,j} & i > j \\ 1 - \sum_{i=1}^{n-1} b_{i,j} & i = n \\ 0 & i \leq j \end{cases} \quad (10)$$

$B_{i,j}$  represents the cumulative weight fraction of material broken from size  $j$  which appears in size interval  $i$ . The subscript 1 refers to the original material of size 1 at time  $t = 0$ , the subscript  $i$  refers to a smaller size than the size  $j$  and the subscript  $j$  refers to the size from which material that appears in size  $i$  is broken. Further, the coefficient  $\emptyset$  can be related to size as:

$$\emptyset = \alpha_1 \cdot \left[ \frac{x_i}{x_1} \right]^{-\delta} \quad (11)$$

where  $\delta$  characterizes the degree of non-normalization.

## 2.2. Experimental

In the recent work, there were two comminution paths tested:

1. Jaw crusher + cone crusher + ball mill
2. Jaw crusher + HPGR + ball mill

In the study, 2.9  $\text{g/cm}^3$  density of ore sample containing 0.8% copper ( $\text{CuFeS}_2$ ) and 0.5 g/t silver ( $\text{AgS}$ ), was the test material. As the first experimental step, an industrial-scale jaw crusher was employed as the primary crushing stage, processing a substantial 75 kg of ore sample. Subsequently,

a cone crusher (CC) and finally a laboratory-scale High-Pressure Grinding Rolls (HPGR) for the pre-grinding stage were used (37.5 for each technology). A representative sample of 1.2 kg from the cone crusher product was obtained using coning-quartering and Jones riffle splitting techniques then was modeled via Weibull double Rossin Rammler model. An exceptional level of precision was achieved in the calculation of mass allocation for each size fraction by taking the advantage of the model. Consequently, it was possible to successfully replicate to the HPGR product size distribution that closely reflecting product size distribution of the cone crusher. sample has the  $P_{80}$  of 8,324  $\mu\text{m}$ . This approach facilitated an examination of the impact of microfractures on mineral behavior by analyzing grinding kinetics by employing population balance approach. The HPGR parameters in the pre grinding stage are shown in Table 1.

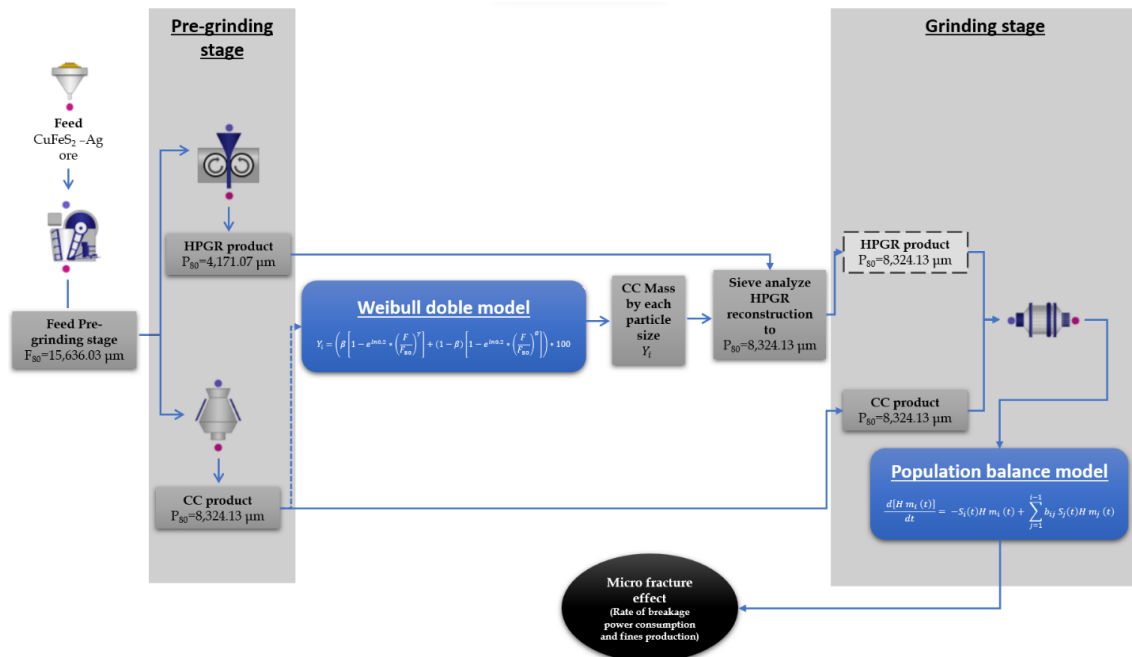


Fig. 3. Experimental and model methodology

Table 1. Industrial jaw crusher parameters

Jaw parameters and operational conditions			
Feed Opening (mm)	900	Crushing velocity (rpm)	293
Close side setting (mm)	60	Capacity (t/h)	75
Crusher power (kW)	75	Specific energy (kWh/t)	0.63

Table 2. HPGR parameters in a pre-grinding stage

HPGR Parameters and operational conditions			
Roller diameter (mm)	1650	Operation gap (mm)	19.32
Roller length (mm)	812	Capacity (t/h)	230.50
Crusher power (kW)	1500	Specific energy (kWh/t)	6.92
Roller velocity (m/s)	1.63	Pressure (bar)	130.20

Table 3. Cone crusher parameters in a pre-grinding stage

Cone crusher Parameters and operational conditions			
Maximum Particle Size (mm)	13.0	Feed hopper assembly (m <sup>3</sup> )	0.019
Final Size (mm)	8.324	Capacity (t/h)	1.2
Crusher power (kW)	150	Specific energy (kWh/t)	2.76

### 2.3. Re-constructing feed size distribution

In this study to correlate the HPGR crushing mechanism and its possible effect on microfractures, the HPGR product was reconstructed to mimic a granulometric product from the cone crusher. The goal of doing this, is to have a similar particle feed size distribution in the process and try to quantify the benefits of possible microfractures for conventional ball milling energy saving. For the granulometric reconstruction, the Double Weibull formula proposed by Rosin Rammler (Zhang and Napier-Munn, 2008; Wills and Finch, 2015) was used. This equation provides a better representation of particle size distribution as compared to single-parameter models like the normal or log-normal distributions. It proves particularly valuable when addressing processes characterized by intricate size distribution patterns that are challenging to discern. The Double Weibull formula is described as follows (Equation 12):

$$Y = \left( \beta \left[ 1 - e^{\ln 0.2 * \left( \frac{F}{F_{80}} \right)^\gamma} \right] + (1 - \beta) \left[ 1 - e^{\ln 0.2 * \left( \frac{F}{F_{80}} \right)^\emptyset} \right] \right) * 100 \quad (12)$$

where  $Y$  is the percent passing in a natural distribution,  $\beta$  refers to the relation between fines and coarse weighting particles factor,  $F_{80}$  is the 80% passing size in the feed ( $\mu\text{m}$ ),  $F$  is the mesh opening size ( $\mu\text{m}$ ),  $\gamma$  refers to the shape factor for the fines and  $\emptyset$  is the shape factor for the coarse fraction. The  $F_{80}$  values for all the tests were proposed according to the distribution; the coarse distribution has a  $F_{80}$  value of 13.808 mm, that of same for the medium and fine distribution functions are 4.826 mm and 0.379 mm, respectively. The value of  $\beta$  approximates to zero as the relation between fine and coarse particle fraction is unknown.

The re-constructed feed size distributions were used instead of the experimental feed size distribution. The amount of ore (g) at each size class was estimated and added, and sieve analyses were carried out for obtaining the data.

### 2.4. Grinding tests

Three grinding time intervals (1, 7.5, and 15 min.) were used in the estimations. The feed size distribution reconstructed by using Equation 2 was maintained in each test and loaded into the mill for batch grinding for the amount that is lost in the tests. After grinding tests were finished, the mill content was discharged, and the particle size analysis was done using screens at  $\sqrt{2}$  interval. The top size for the product was 8,324  $\mu\text{m}$  and the lowest size was 38  $\mu\text{m}$ . Tests were repeated as explained for the cone crusher and HPGR.

The laboratory mill has a diameter of 0.32 m with 0.35 m in length. The charge level and solid by weight were set to 40% and 68% for all tests, respectively. The rated power of the mill motor was 2.23 kW and includes a variable speed controller unit that was used to set the mill speed to 48.6 rpm (65% of Nc). The digital rpm counter was used to verify the rotational speed of the mill. The voltage and amperage measured during the grinding were used to calculate the power consumption. A GGS (Gates-Gaudin-Schuhmann) model was used to decide at the ball distribution in the mill. The parameters and experimental data are shown in Table 4 and Table 5.

## 3. Results and discussion

### 3.1. Sample parameters determination

Fig. 4 shows the sieve analysis for the pre-grinding stage that consists of submitting the jaw crusher product to the cone crusher and HPGR.  $F_{80}$  of the jaw product was 15,636  $\mu\text{m}$ . The  $P_{80}$  of the product obtained using the conventional cone crusher and HPGR were 8,324  $\mu\text{m}$  and 4,171  $\mu\text{m}$ , respectively as expected, the HPGR technology provided the lower  $P_{80}$  value. Table 6 shows the reduction ratio (RR) (feed size  $F_{80}$  to the product size  $P_{80}$ ). It is also used as an indicator of the proportional reduction of the crusher (Taggart and Behre, 1945). The RR values of cone crusher and HPGR are 1.88 and 3.75, respectively.

### 3.2. Re-constructed feed size distribution

Using Rosin Rammler's Weibull double (Equation 12) it was possible to use the cone crusher product as a reference to recreate a new HPGR sieve analysis.; it was possible determine the mass in each sieve

class, then construct an experimental new size distribution. The principal objective was to feed the same particle size distribution (-1500 +41.31  $\mu\text{m}$ ) to the ball mill grinding process regardless of the type of technology (either cone crusher or HPGR technology). For this case, the necessary mass to obtain 40% charge level in the mill was approx. 8.35 kg. Fig. 5 shows the cone crusher size distribution and HPGR reconstructed size distribution via modelling. Table 7 shows the parameters used in Equation 12.

Table 4. Experimental data

<b>Motor Power (Hp)</b>	3	<b>Ore type</b>	CuFeS <sub>2</sub> -Ag
<b>D (m)</b>	0.32	<b>W<sub>B</sub> (kWh/t)</b>	18.56
<b>Length (m)</b>	0.35	<b>F<sub>80</sub> (<math>\mu\text{m}</math>)</b>	8,324
<b>Level Charge (%)</b>	40	<b>Critical Speed (%)</b>	65

Table 5. Distribution parameters vs ball size distribution

Gates-Gaudin-Schuhmann model ( $m=4.8$  is the slope of lineal distribution;  $k_{100}=76.6$  is the top size in the distribution,  $x_i$  is the reference ball size, where the model is defined as  $(x_i/k_{100})^m$ )

Ball Size (mm)	Cumulative Distribution (%)
76.6	100%
63.5	41%
50.8	14%

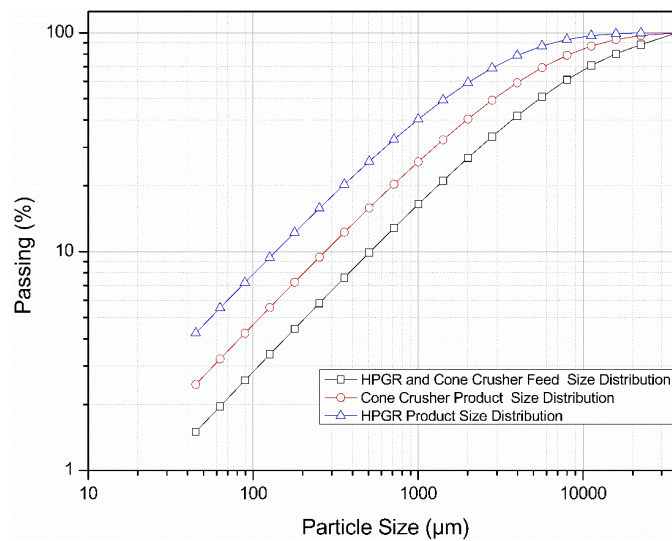


Fig. 4. Size Analyses of feed the products

Table 6. RR values to cone crusher and HPGR technology

Reduction Ratio (RR)	
Cone Crusher	1.88
HPGR technology	3.75

### 3.3. Grinding results: specific energy and power consumption

The initial stages involve pre-grinding using High-Pressure Grinding Rolls (HPGR) and a Cone crusher, with the subsequent processing taking place in a ball mill. In Figs. 6 and 7, the particle size distributions of the feed and the products from the cone crusher and HPGR are illustrated at 1, 7.5, and 15-minute intervals of grinding. A high proportion of fine fraction was observed in HPGR compared to the cone crusher. The product from the HPGR at a grinding time of 15 min. has a  $D_{80}$  value of 1,114  $\mu\text{m}$  while the

cone crusher denotes a  $D_{80}$  of 1,742  $\mu\text{m}$ . Table 9 shows the specific energy values for each technology. As mentioned above there are two size reduction paths in this study before the grinding stage:

1. Jaw crusher + cone crusher + ball mill
2. Jaw crusher + HPGR + ball mill

Particle weakening by HPGR may be explained by the lower specific energy consumption of the ball mill in the downstream process that is 12.46 kWh/t (after 15 min grinding). However, for the first size reduction path the ball mill specific energy consumption is 14.36 kWh/t (after 15 min grinding). On the other hand, the total energy consumption for the first and second paths are 17.75 and 17.02 kWh/t, respectively. The HPGR specific energy consumption itself is 3.93 kWh/t. The specific energy consumption in all the comminution processes is showing in Table 8.

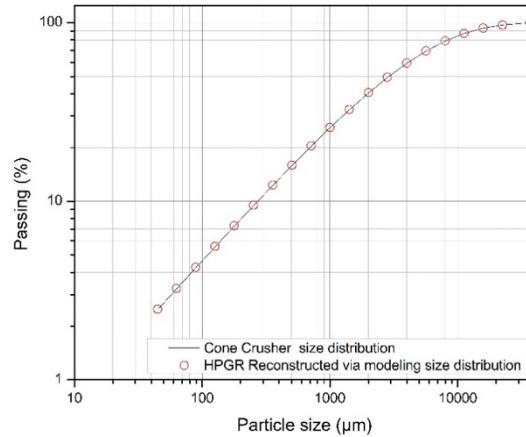


Fig. 5. Cone crusher and HPGR feed size distribution to mill stage

Table 7. Weibull double parameters formula

Parameters	$\beta$	$F_{80}(\mu\text{m})$	$\gamma$	$\phi$
Cone Crusher	0.0712	8324.13	0.8165	0.796

Table 8. Specific energy in comminution stage

	Specific energy (kWh/t)			Total specific energy in comminution stage (kWh/t)
	Jaw Crusher	Cone Crusher	Ball Mill	
1	0.63	2.76	14.36	17.75
2	0.63	3.93	12.46	17.02

### 3.4. Effect of the HPGR technology versus cone crusher on breakage rates and fines generations

The Fig. 8 shows the rate of breakage for ball milling due to each pre grinding stage (using HPGR and cone crusher). The HPGR technology has the higher rate of breakage ( $0.00209 \text{ min}^{-1}$ ) under the proposed conditions. The cone crusher has the rate of breakage value of  $0.00103 \text{ min}^{-1}$ . Some researchers explained in their studies (Genç and Benzer, 2016; Altun *et al.*, 2011) that supports our conclusion that HPGR technology increases the rate of breakage thus specific energy consumption of the system is decreased. In the context of the study outlined in this paper, it can be deduced that the primary driver behind the enhancement in grinding performance does not only results from the reduction in feed size. In addition, it appears that the optimization of grinding can be enhanced by the generation of microfractures during a compression event, a phenomenon closely linked to the utilization of HPGR technology. The estimated parameters for  $S_i^E$  and  $B_{ij}$  are shown in Tables 10 and 11, respectively. The  $B_{ij}$  values were calculated using the “zero order production of fines” method (Herbst and Fuerstenau, 1968)

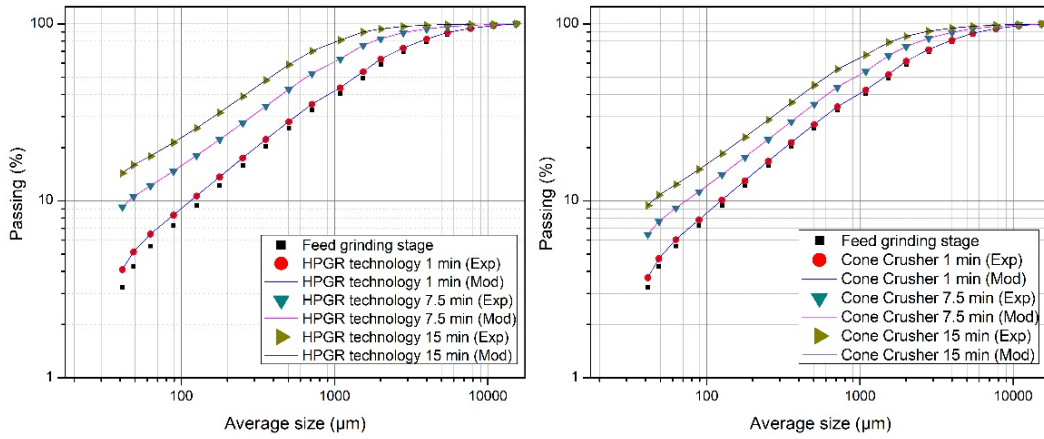


Fig. 6. Ball mill grinding sieve analyses and modeling of HPGR technology (left) and cone crusher (right)

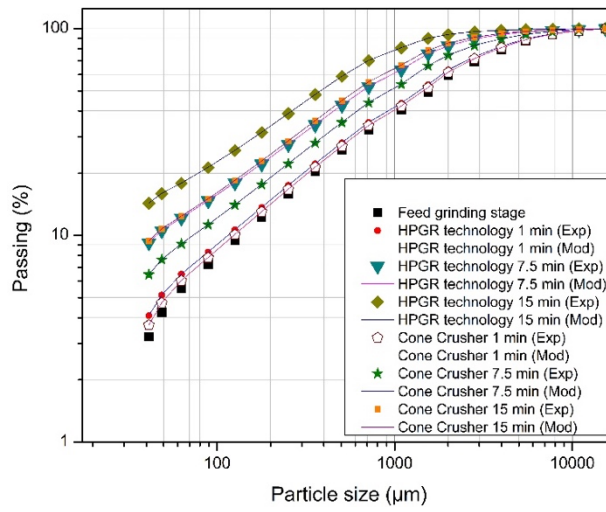


Fig. 7. Comparison of ball mill grinding sieve analyses and modeling of HPGR technology and cone crusher

Table 9. Ball mill specific energy consumption after HPGR and Cone crusher

Specific energy (kWh/t)	
HPGR technology	12.46
Cone Crusher	14.36

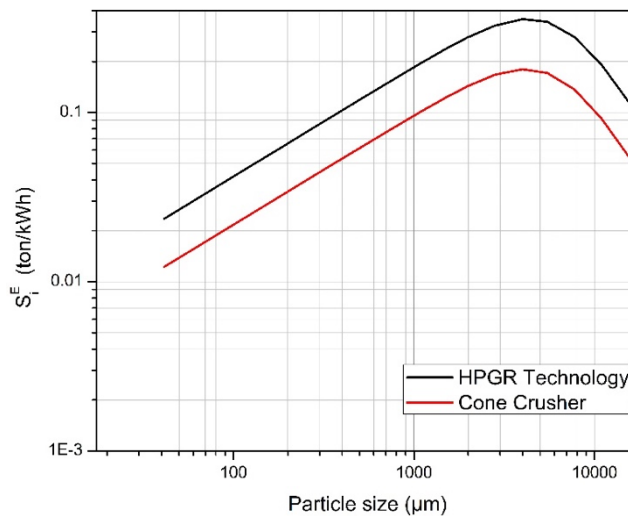


Fig. 8. Rate of breakage to cone crusher and HPGR technology grinding kinetics

Table 10.  $S_i^E$  values to HPGR technology and cone crusher.

Parameters	Specific Selection Function				
	$S_1^E$	$a$	$\alpha$	$\Lambda$	$\mu$
Units	(t/kWh)	min <sup>-1</sup>	---	---	$\mu\text{m}$
HPGR technology	0.1160	0.00209	0.650	2.5	6531.99
Cone Crusher	0.0552	0.00103	0.649	2.5	6300.01

Table 11.  $B_{ij}$  Calculated parameters.

Parameters	$\alpha_1$	$\alpha_2$	$\alpha_3$
HPGR technology	0.123	0.250	4.0
Cone Crusher	0.103	0.240	3.9

Fig. 9 shows the dimensionless size curve that is normalized by median size,  $X_{50}$ . The self-similarity of the distributions is observed in the graphs. HPGR aided grinding sizes curve is finer than the cone crusher aided one. This trend is maintained throughout the grinding process other than 30-60% and 75-85% regions. This behavior may be explained that due to the feed size, used in the grinding the particles between 0.5 and 1.3 values of  $X/X_{50}$  have the same generation rate. Combining Fig. 8 and 9, it may be possible to conclude that the rapid coarse particles reduction by HPGR technology, helps to generate a larger number of fine particles with low specific energy consumption as compared to the cone crusher aided grinding case.

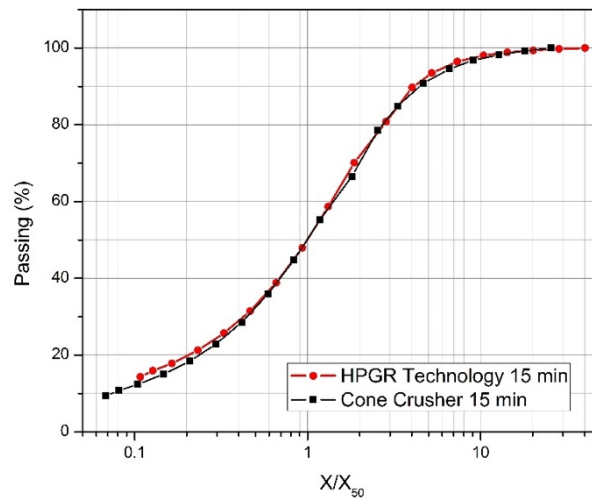


Fig. 9. Ball mill grinding cumulative passing (%) vs normalized product size distributions ( $X/X_{50}$ ) for Cone Crusher and HPGR technology grinding kinetics

#### 4. Conclusions

In this paper two different size reduction paths were studied:

1. Jaw crusher + cone crusher + ball mill
2. Jaw crusher + HPGR + ball mill

by using Rosin Rammler's Weibull double formula and the population balance model together. The aim was trying to understand and quantify the particle weakening effect due to HPGR fracture mechanism. To understand and quantify the effect:

- the reduction ratio,
- the breakage rates,
- the specific energy consumption of the downstream ball mill process, were investigated.

Consequently, the following conclusions were drawn from the study.

- The ball mill sieve analyses after 15 min shows that the the HPGR case has the higher reduction ratio ( $D_{80}$  value is 1,114  $\mu\text{m}$  while the cone crusher  $D_{80}$  is 1,742  $\mu\text{m}$ ),
- HPGR aided ball mill grinding path results in lower specific energy consumption with a greater reduction ratio.
  - Jaw crusher (0.63 kWh/t) + cone crusher (2.76 kWh/t) + ball mill (14.36 kWh/t) = 17. 75 kWh/t
  - Jaw crusher (0.63 kWh/t) + HPGR (3.93 kWh/t) + ball mill (12.46 kWh/t) = 17.02 kWh/t
- HPGR technology has the higher rate of breakage ( $0.00209 \text{ min}^{-1}$ ) as compared the cone crusher ( $0.00103 \text{ min}^{-1}$ ).
- The weakening effect helping ball mill grinding due to microfractures created using HPGR can be justified in this study by:
  - by maintaining a constant feed size distribution during the ball mill grinding stage (achieved through the application of the Rosin Rammler's Weibull double model),
  - considering the higher rate of breakage for HPGR estimated via PBM,
  - fine generation (as depicted in Fig. 9), and
  - lower specific energy consumption of HPGR.

### Acknowledgments

The authors thank to the mining company Grupo México, the SEP (Secretary of Public Education) and the Institute of Metallurgy of the UASLP for the facilities provided to carry out this project.

### References

- AUSTIN, L., 1972. *Estimation of non-normalized breakage distribution parameters from batch grinding*. Powder Technol. 5 (5), 267-277.
- AUSTIN, L.G., BRAME, K., 1983. *A comparison of Bond method for sizing wet tumbling ball mills with a size-mass balance simulation model*. Powder Technol. 34 (2), 261-274.
- AUSTIN, L.G., 1982. *Rate equations for non-linear breakage in mills due to materials effects*. Powder Technol. 31, 127-133.
- ALTUN OKAY, BENZER HAKAN, DUNDAR HAKAN, AYDOGAN NAMIK A., 2011. *Comparison of open and closed circuit HPGR application on dry grinding circuit performance*, Minerals Eng., 24(3-4), 267-275.
- CELIK, I.B., ONER, M., 2006. *The influence of grinding mechanism on the liberation characteristics of clinker minerals*. Cem. Concr. Res. 36 (3), 422-427.
- DANIEL, M., 2007. *Energy efficient mineral liberation using HPGR technology*. PhD thesis University of Queensland, JKMRRC, Australia.
- DATTA A. *A model of batch grinding with impact energy spectra*. Ph.D. Thesis, Department of Metallurgical Engineering, University of Utah, 1999.
- DHAWAN, N., SAFARZADEH, M. S., MILLER, J. D., MOATS, M. S., RAJAMANI, R. K., LIN, C. L. (2012). *Recent advances in the application of X-ray computed tomography in the analysis of heap leaching systems*. Minerals Engineering, 35, 75-86
- DUNNE, R., GOULSBRA, A., DUNLOP, I., 1996. *High-pressure grinding rolls and the effect on liberation: comparative test results*. Randol Gold Forum 49-54.
- FAN, J.J., QIU, G.Z., JIANG, T., GUO, Y.F., HAO, H.Z., YANG, Y.B., 2012. *Mechanism of high-pressure roll grinding on compression strength of oxidized hematite pellets*. J Central South Univ 19 (9), 2611-2619.
- FUJIMOTO, S., 1993. *Reducing Specific Power usage in Cement Plants*, vol. 7. World Cement, pp. 25-35.
- GUO, X.; CUI, S., DAI, S., HAN, J., WANG, C. (2019). *Investigation of microcrack formation in vanadium-titanium magnetite using different crushing processes*. J. South. Afr. Inst. Min. Metall. 2019, 119, 811-816.
- GUTSCHE, O., FUERSTENAU, D.W., 2004. *Influence of particle size and shape on the comminution of single particles in a rigidly mounted roll mill*. Powder Technol. 143 (26), 186-195.
- GENÇ, Ö., BENZER, A.H., 2016. *Effect of High-Pressure Grinding Rolls (HPGR) pre-grinding and ball mill intermediate diaphragm grate design on grinding capacity of an industrial scale two-compartment cement ball mill classification circuit*, Minerals Eng. 92, 47-56,
- HERBST, J.A., FUERSTENAU, D.W., 1973. *Mathematical simulation of dry ball milling using specific power information*. Trans. SME - AIME 254, 343-348.

- HERBST, J.A., FUERSTENAU, D.W., 1968. *The zero order production of fine sizes in comminution and its implication in simulation*. Trans. Am. Inst. Min. Eng. 241 (1968), 538–549.
- HERBST, J.A., RAJAMANI, R.K., MULAR, A.L., JERGENSEN, G.V., 1982. *Developing a Simulator for Ball Mill 1986 Scale-Up: A Case Study. Design and Installation of Comminution Circuit*. AIME, New York, pp. 325–345.
- KATUBILWA, F.M., MOYS, M.H., 2009. *Effect of ball size distribution on milling rate*. Miner. Eng. 22, 1283–1288.
- KING, R.P., 2001. *Modeling and Simulation of Mineral Processing Systems*. Butterworth-Heinemann ISBN 0-7506-4884-8.
- KLIMPEL, R.R., *Slurry Rheology Influence on the performance of Mineral/Coal Grinding Circuits*, Mining Eng., 1983, 21–28.
- MAXTON, D., MORLEY, C., BEARMAN, R.A., 2003. *Quantification of the benefits of high-pressure rolls crushing in an operating environment*. Miner. Eng. 16 (9), 827–838.
- MICHAELIS, V.H., 2005. *Real and potential metallurgical benefits of HPGR in hard rock ore processing*. In: Proceedings of the Randol Innovative Metallurgy Forum Held in Perth, W.A., Australia, 21–24 August, pp. 31–39.
- MILLER, J., LIN, C.-L. (2009). *Recent Advances in Mineral Processing Plant Design*. In A. L. Mular, D. N. Halbe, & D. J. Barratt (Eds.), Mineral Processing Plant Design, Practice, and Control: Proceedings, Volume 1 (pp. 48–59). Society for Mining, Metallurgy, and Exploration (SME).
- NGHIPULILE, T., NKWANYANA, S., LAMECK, N. (2023). *The Effect of HPGR and Conventional Crushing on the Extent of Micro-Cracks, Milling Energy Requirements and the Degree of Liberation: A Case Study of UG2 Platinum Ore*. Minerals 2023, 13, 1309.
- NOMURA, S., HOSODA, K., TANAKA, T., 1991. *An analysis of the selection function for mills using balls as grinding media*. Powder Technol. 68, 1.
- SCHONERT, K., 1988. *A first survey of grinding with high-pressure compression roller mills*. Int. J. Miner. Process. 22 (1–4), 401.
- TAVARES, L.M., CARVALHO, R.M., 2009. *Modeling breakage rates of coarse particles in ball mills*. Miner. Eng. 22 (7–8), 650–659.
- TAVARES, L.M., 2005. *Particle weakening in high-pressure roll grinding*. Miner. Eng. 18 (7), 651–657.
- TUZCU, E.T., RAJAMANI, R.K., 2011. *Modeling breakage rates in mills with impact energy spectra and ultra-fast load cell data*. Miner. Eng. 24, 252–260.
- TAGGART, A. F., BEHRE H. A., 1945. *Handbook of Mineral Dressing, Ores and Industrial Minerals*, Volume 1. Wiley J. & sons, Incorporated, 1905 pp.
- VOGEL, L., PEUKERT, W., 2003. *Breakage behaviour of different materials-construction of a mastercurve for the breakage probability*. Powder Technol. 129, 101–110.
- WILLS, B. A., FINCH, J. A. (2015). *Wills' mineral processing technology: an introduction to the practical aspects of ore treatment and mineral recovery*. Elsevier.
- ZHANG, J., NAPIER-MUNN, T. J. (2008). *Comminution handbook*. Julius Kruttschnitt Mineral Research Centre, The University of Queensland.
- ZHAO, X., HUANG, S., LIU, C., DENG, L., 2011. *Study on the crush model of high-pressure grinding rolls*. Electr. Inf. Eng. Mechatron. 921–928.